

# Influence of Heat Treatment Parameters on Magnetic Properties of Non-oriented electrical Steels

Y. Sidor<sup>1</sup>, F. Kováč<sup>1</sup>, L. Novák<sup>2</sup>, J. Kravčák

<sup>1</sup>Institute of Materials Research of Slovak Academy of Sciences, Watsonova 47, 043 53 Kosice, Slovakia

<sup>2</sup> Department of Physics of Technical University, Park Komenského 2, 04200 Košice, Slovakia

\*Corresponding author; e-mail: sidor@imrnov.saske.sk

## Abstract

Decarburising annealing in the two-phase region is a known method to provide the columnar grain growth in silicon non-oriented electrical steel. This method includes long term pre-heat treatment in vacuum and subsequent decarburising annealing in the wet hydrogen atmosphere [1].

This paper describes alternative method to produce the columnar microstructure in the middle silicon non-oriented electrical steel without pre-heat vacuum annealing. The influence of applied annealing temperature and atmosphere on the development microstructure are studied under the conditions of industrial continuous annealing. Dependence of the final material texture on the aforementioned conditions is presented.

## Introduction

The advantages of the cube texture in the electrical steel sheets have already been recognized during the past century.  $(100)\langle 001 \rangle$  and  $(100)\langle uvw \rangle$  textures are “ideal” ones for the grain oriented and non-oriented electrical steel respectively. But the nature of the cube-oriented grains growth does not permit production of such textured steel sheets by applying conventional rolling and annealing processes.

Assumes pointed out first that high temperature annealing of very thin Si-Fe sheets leads to an abnormal growth of the cube grains [2]. In this case, the secondary recrystallisation process of the cube-oriented grains is controlled by the gas-metal interfacial energy, which is the lowest at the  $(100)$  orientation in the high purity inert atmosphere or in vacuum [3-5]. Other possible method to increase the ratio of the cube-oriented grains is cross rolling and subsequent high temperature annealing [6]. Another recently developed process of the cube-oriented grain growth in the silicon steels consists of manganese removing annealing in vacuum and subsequent decarburising annealing in the  $\gamma$  or  $\alpha+\gamma$  two phase region in decarburising atmosphere [1,7,8] or high-temperature annealing in vacuum with application of the oxide separator in between the sheets [9]. Nevertheless, all of the described methods cannot be applied in the industrial practice.

The later process itself is diffusion-controlled  $\alpha+\gamma \rightarrow \alpha$  phase transformation in the surface layer and subsequent abnormal growth of the ferrite “surface” grains into the two-phase matrix towards the middle plain of the sheet as the result of decarburisation. This “abnormal” grain growth, enhanced by the decarburisation process, is responsible for the formation of columnar microstructure [10]. The columnar microstructure can also be formed during the reverse process of the carburisation when austenitic columnar grains are growing. If the decarburisation/carburisation process is observed in the binary *Fe-C* system, then growth of columnar grains take place without the formation of the transient two-phase zone. In the case of the ternary *Fe-C-Si* system, probably the austenite+ferrite transition zone is be formed. Formation

of the  $\alpha+\gamma$  region is expected during the carburisation, even if the content of  $Si$  is minimal. Contrary to carburisation, during the decarburisation the two-phase region might not be formed even at high content of  $Si$  [11]. According to [12], the columnar microstructure in the steels is formed only if the decarburisation annealing is performed in the  $\alpha+\gamma$  region and the sharp interface exists between the decarburised ferrite and the two-phase area.

It is expected that formation of the columnar microstructure is formed when the velocity of the transformation front is higher than the rate of nucleation [13]. Apart from the decarburisation, the temperature gradient in material can provide conditions for the growth of columnar ferrite grains [14]. Nevertheless, the decarburisation process in the two-phase region can be efficient controlling mechanism to obtain an alternative mechanism of columnar ferrite microstructure in the solid state.

Decarburisation in steel can be described according to the reactions [13]:



The temperature range for reaction (1), (2) and (3) are  $T=670-690^\circ\text{C}$ ,  $T>700^\circ\text{C}$  and  $T<530^\circ\text{C}$  respectively. Non-oriented electrical steel sheets, regardless of production type, i.e. semi- or fully-proceed, are annealed usually during the final annealing in the temperature range where equation (2) is valid. The use of wet atmosphere is inevitable for the effective decarburisation, because rate of the chemical reaction (2) is proportional to the so-called an oxidation potential  $p_{H_2O}/p_{H_2}$ . Optimum value of the oxidation potential of the decarburising atmosphere (if  $p_{H_2}/p_{N_2} \geq 0.5$ ) is  $\sim 0.5$  [15].

Theory of decarburisation kinetic in which phase transformation (i.e.  $\gamma \rightarrow \alpha$  or  $\alpha+\gamma \rightarrow \alpha$ ) is involved was developed by Wagner [16], Swisher [17] and Pyyry and Kettunen [18]. For the case of Fe-C alloy an the initial microstructure of  $\alpha+\gamma$  at the decarburisation temperature  $Ar_1 < T < Ar_3$ , the following equation is valid [17,18]:

$$\bar{C} = C_i - \frac{1}{a} \sqrt{\frac{6D_f C_b t}{3C_i - bC_b} \left( C_i - \frac{C_b}{2} \right)} \quad (4)$$

where  $\bar{C}$  is average carbon concentration after the decarburisation (in wt.%),  $C_i$  is the initial carbon concentration,  $a$  is the sheet half-thickness in cm,  $D_f$  is a diffusion coefficient of the carbon in the ferrite in  $\text{cm}^2/\text{s}$ ,  $C_b$  is the carbon concentration in the ferrite equilibrium with the austenite,  $t$  is time in seconds and constant  $b=2$  [17] or  $b=3$  [18]. According to [17] and [19]:

$$D_f = 0.256 e^{-24200/RT} \quad (5)$$

$$C_b = 0.1395 - 1.099 \times 10^{-4} T \quad (6)$$

where  $R$  is the universal gas constant and  $T$  is the temperature.

If the initial microstructure is  $\gamma$ , rather than  $\alpha+\gamma$ , the decarburisation develops a concentration gradient in  $\gamma$ , and then the following equation is applied [17]:

$$\bar{C} = C_i - \frac{1}{a} \left[ 2kC_a \sqrt{D_f t} + \frac{1.128(C_i - C_a) \sqrt{D_a t} \exp(-k^2 D_f / D_a)}{1 - \text{erf}(k \sqrt{D_f / D_a})} \right] \quad (7)$$

where  $C_a$  is the carbon concentration in the austenite equilibrium with the ferrite, and  $D_a$ , the diffusion coefficient of the carbon in the austenite in  $\text{cm}^2/\text{s}$ , is:

$$D_a = [0.07 + 0.06 (C_i)]e^{-32000/RT} \quad (8)$$

$k$  is a function of  $C_i$  and  $T$  and can be established empirically.

According to the Ref. [20], maximum decarburisation rate at app.  $816^\circ\text{C}$  is virtually independent of the initial  $C$  content. The decrease of the decarburisation rate at  $T > 816^\circ\text{C}$  can be explained as transition from the internal oxidation mode to the external one [21].

At lower temperatures (internal oxidation), there is the base metal matrix available for the diffusion of the carbon to the surface of the material. At  $T \sim 810\text{-}820^\circ\text{C}$ , the initiation of the external oxidation is observed, when a continuous oxide layer is present at the oxidation front, that inhibits the diffusion of the carbon to the surface and its removal.

Hence, the annealing temperature as well as the content and the dew point of the decarburising atmosphere are crucial factors that influence developing of the columnar microstructure during the decarburisation in the two-phase region. The main goal of present work was to find the optimum conditions for obtaining of the proper columnar microstructure with depressed deformation and increased cube or near-cube texture components.

## Experiment

Both semi-proceed (SP) and fully-proceed (FP) types of the electrical non-oriented steels were used for the experiment (see Tab. 1).

Table 1. Chemical composition of steel, in wt. %.

steel	C	Mn	Si	P	S	Al	N
SP	0.05	0.36	0.24	0.068	0.008	0.109	0.005
FP	0.03	0.38	1.01	0.134	0.008	0.157	0.007

Thickness of both SP and FP sheets were  $h=0.65$  mm. Samples of both steels were annealed in the decarburising atmosphere consisted of 35% of  $H_2$  and 65% of  $N_2$  with the dew point of  $35^\circ\text{C}$ . SP steel samples were taken from the industrial link after the temper rolling and samples of FP – after the cold rolling.

The samples were annealed according to the “stair-temperature” schedule (see Fig. 1) in the intercritical region. Three different heating rates  $V_1 > V_2 > V_3$  to the  $T_1$  temperature were applied with fixed  $T_1$ ,  $T_2$ ,  $\tau_1$  and  $\tau_2$ . At  $T_1$  after  $\tau_1$  the material should have the fine primary recrystallised microstructure and the thin decarburised  $\alpha$ -region on the sheet surface;  $T_1$  varies according to the chemical composition of material.  $T_2$  was chosen with the aim to provide the efficient decarburisation of the material and was the same for both steels. Total time of the annealing was chosen in accordance to industrial condition of continuous annealing. Both steels laboratory prepared columnar states were compared with the corresponding industry produced ones.

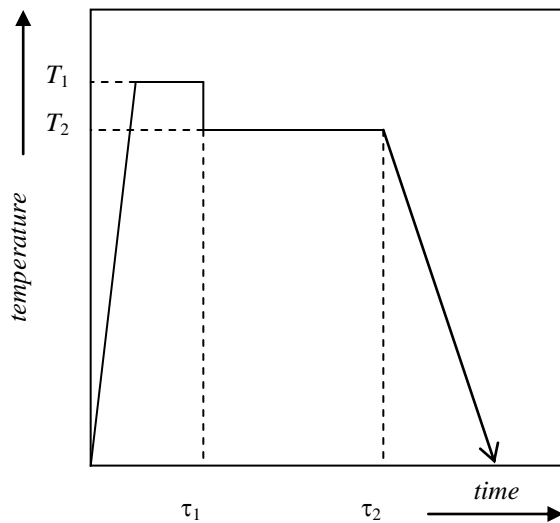


Fig. 1. Schedule of anneal in two-phase region

The texture was measured by the means of EBSD utilising Orientation Imaging Microscopy (OIM™) software package.

## Results and discussion

After the completed primary recrystallisation, a strong texture gradient is observed in both steels in the plain of cross section. In Fig. 2, SP steel ODFs at  $\varphi_2 = 45^\circ$  in the state after the primary recrystallisation in the middle plain and in the plain near the sheet surface are compared. It is obvious, that near surface the texture has developed strong  $\theta'$ -fibre and weak (110)[1-11] peak, and contrary to this, the texture in the middle plain has strong J-component (114)[1-10]. Therefore during the subsequent secondary recrystallisation process enhanced by the decarburisation, when pronounced grain growth takes place from the surface region towards the

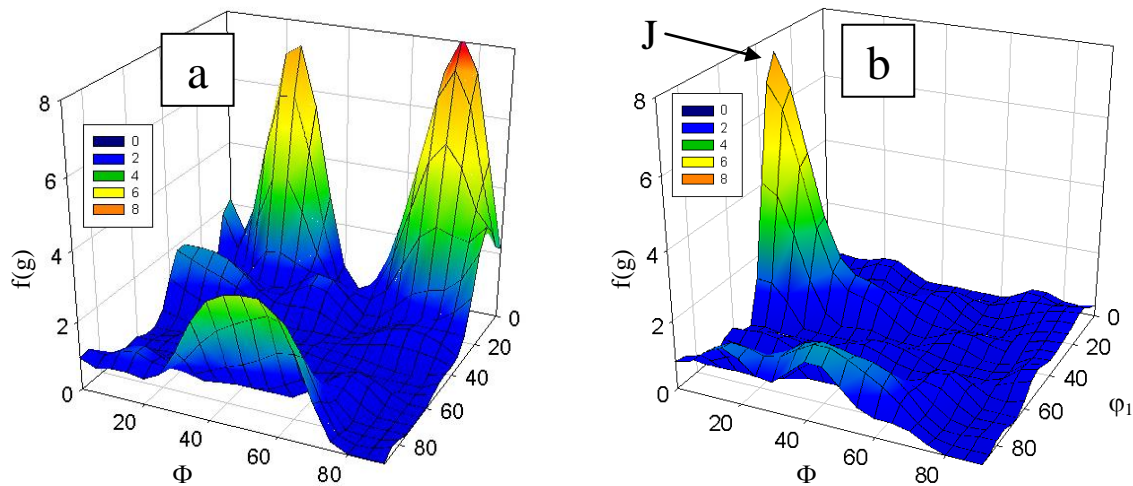


Fig. 2. ODF of SP steel after primary recrystallisation,  $\varphi_2 = 45^\circ$ : a) subsurface at 1/8 of sheet thickness; b) middle sheet plain.

middle sheet plain, it is possible to expect strong cubic/near cubic texture component in the final state. In Fig. 3a and 3b, development of the columnar microstructure in the SP steel during “columnar” annealing with the optimum heating rate  $V$  is shown. Sample in Fig. 3a was taken after the finish of the 1<sup>st</sup> stage of the annealing ( $T_1$ ,  $\tau_1$ ).  $T_1$  was chosen to provide the fine homogeneous microstructure with the certain amount of  $\gamma$ -phase at the beginning of the first stage. During this stage the decarburisation promotes the growth of the ferrite columnar grains from the surface region towards the two-phase middle region of the sheet. After finishing of the decarburisation process at  $T_2$ , the microstructure is fully ferritic and grains have columnar shape (see Fig. 3b). Highly non-stable conditions of grain growth near the sheet surface leads to the formation of the thin layer of inhomogeneous relatively fine microstructure on the steel surface.

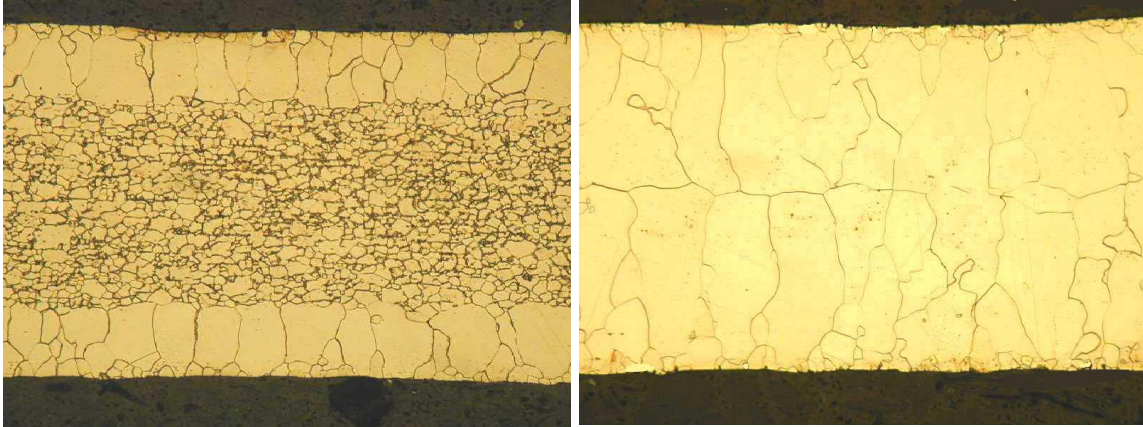


Fig. 3. Microstructure of samples of SP steel: a) at the commence of ( $T_2, \tau_2$ ) part of columnar anneal; b) after columnar anneal. Magn.x70

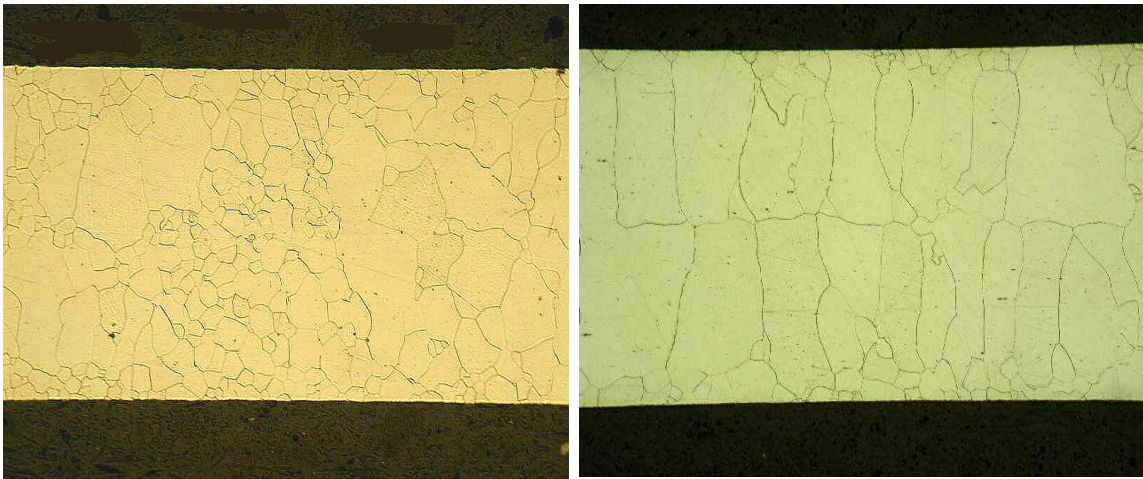


Fig. 4. Microstructure of samples of FP steel: a) after columnar anneal with heating rate of  $V_2$  on  $T_1$ ; b) after columnar anneal with heating rate of  $V_1$  on  $T_1$ . Magn.x70

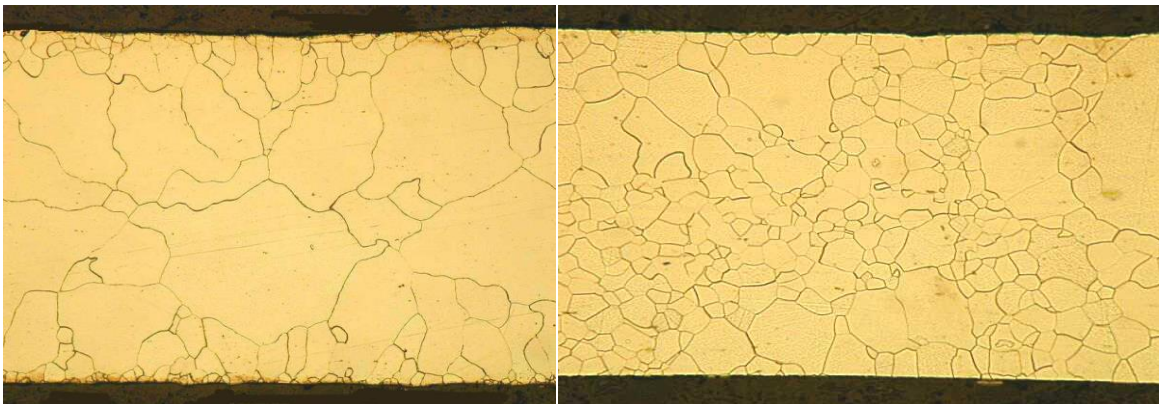


Fig. 5. Microstructure of samples: a) SP steel after customer anneal according to EN 10 126/95; b) FP steel after continuous industrial anneal. Magn.x70

Microstructure of the same SP steel annealed according to the EN 10 126/95 has polygonal and highly inhomogeneous microstructure (see Fig. 5a).

In Fig. 4, the influence of the heating rate  $V$  ( $V_1 > V_2$ ) during annealing of FP steel in the intercritical region according to the schedule in Fig.1 on microstructure is studied. If material is heated with low heating rate  $V_2$ , simultaneously with the decarburisation, intensive normal grains growth is proceed, and final material has the inhomogeneous polygonal microstructure (Fig. 4a). If heating on  $T_1$  is realised with high heating rate  $V_1$  and time  $\tau_1$  of holding at  $T_1$  is short, at  $T_2$ , instead of the equiaxial grain growth, the abnormal columnar grain growth, assisted by decarburising process, is observed (Fig. 4b). The same material annealed under the industry conditions has the polygonal inhomogeneous microstructure (Fig. 5b) similar to the laboratory-annealed steel in the two-phase region with low heating rate on  $T_1$ .

The final state texture was measured on the cross-section of samples. In the case of fine polygonal microstructure (mean grain size  $\approx 40 \mu\text{m}$ ) the ODF was calculated from area of  $0.65 \times 1.47 \text{ mm}^2$ . For a complete description of columnar microstructure texture's the data from 6 random cross-sections of  $0.65 \times 1.47 \text{ mm}^2$  were collected, and ODF was created from the merged data of 6 areas. In Fig. 6, ODF at  $\varphi_2 = 45^\circ$  of FP steel sample with the columnar microstructure is compared with corresponding ODF of the same steel (industrial made) of the polygonal

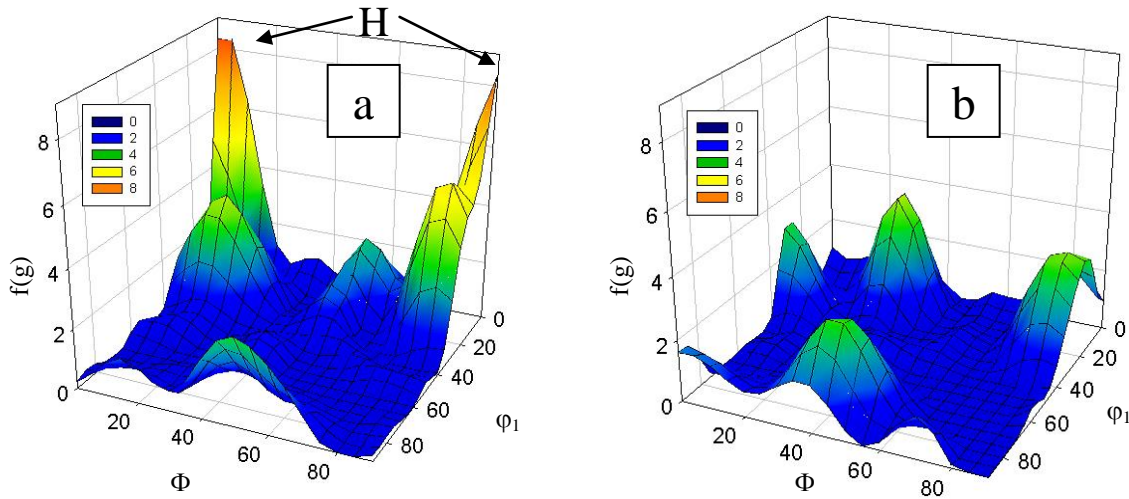


Fig. 6. ODF of FP steel after anneal,  $\varphi_2 = 45^\circ$ : a) sample with columnar microstructure, laboratory experiment; b) sample with polygonal microstructure, industrial processing

microstructure. Texture of the former sample has strong cubic H-component (001)[1-10] and weak developed J component (114)[1-10]. Texture of latter one is fairly random with weak non-uniform developed  $\theta'$ -fibre, weak J component and weak (110)[1-11] peak. Hence, the intensity of the cubic orientation is higher in the sample with the columnar microstructure. Increasing the cubic component intensity the magnetic properties improved (see Tab.2). The same results observed in [22].

Table 2. Electromagnetical properties of steels under investigation.

Steel	Columnar microstructure, laboratory annealing		Polygonal microstructure, industrial annealing	
	$B_{25}$ , T	$P_{1.0}$ , W/kg	$B_{25}$ , T	$P_{1.0}$ , W/kg
SP	1.69	2.05	1.65	2.53
FP	1.7	1.95	1.66	2.95

Generally, after the primary recrystallisation material under the investigation has the highest density of cube/near cube oriented grains not right on the surface, but at the some minimal depth. To increase the probability of the selective abnormal growth of the cube-oriented primary recrystallised grains enhanced by the decarburisation process, it is necessary to establish the optimum conditions of the cold/temper rolling, i.e. radius of rolls, value of reduction, roughness of rolls, etc., which dramatically influence the primary recrystallisation process in the non-oriented electrical steel [23-25]. Those optimum conditions of cold deformation should provide the wide band of the cube-oriented primary recrystallised grains as close to steel surface as it is possible.

Other possible way to increase the probability of the abnormal growth of the cube grains in the primary recrystallised matrix is correction of the annealing regime in the intercritical region. Under specific conditions of the decarburisation in the two-phase region, it is possible to expect the creation of the consistently growing ferrite zones “inside” of the two-phase region (deeper than  $\alpha/\alpha+\gamma$  front) due to the intensive re-distribution of *C* and *Si* atoms near the surface of the sheet [11]. In such situation, the “nucleation” of the abnormal grain growth at some sheet depth increases probability that the abnormal growing ferrite grains have the cube orientation.

Another process, that could increase the probability of the abnormal growth of cubic grains, is proper chemical treatment of the steel surface, which should prevent/decrease the rate of the decarburisation process of the non-cube-oriented primary recrystallised grains.

## Summary

1. Proposed “two-step” decuburising continuous annealing process in the intercritical region of the non-oriented electrical steels with either low or middle content of *Si* leads to the columnar microstructure of the final sheet.
2. Texture of the columnar microstructure has more pronounced cube component compared to the same steel with the polygonal microstructure.
3. The efficiency of the development of the columnar microstructure with preferable cube orientation can be increased by the optimisation of the cold/temper rolling parameters, application of proper regime of decarburising annealing in the intercritical range or by the special chemical treatment of the steel surface before annealing.

## Acknowledgement

This work was supported by the Slovak Grant Agency VEGA, project No. 2/1063/21

## References

- [1] Tomida, T. and Tanaka, T. (1995). *ISIJ Int.*, 35, p. 548.
- [2] Assumus, F., Detert, K. and Ibe, G. (1957). *Zur. Metallk.*, 48, p. 344.
- [3] Detert, K. (1959). *Acta Metall.*, 7, p. 589.
- [4] Walter, J. L. (1959). *Acta Metall.*, 7, p. 424.
- [5] Walter, J. L. and Dunn, C.G. (1960). *Trans. Metall. Soc. AIME*, 218, p. 914.
- [6] Taguchi, S. and Sakakura, A. (1968). *Kinzoku Butsuri (in Japanese)*, 7, p. 221.
- [7] Tomida, T. (1996). *J. Appl. Phys.*, 79, p. 5443.

- [8] Tomida, T. (1996). *J. Mat. Eng. Perfor.*, 5, p. 316.
- [9] Tomida, T., Sano, N., Ueda, K., Fujiwara, K. and Takahashi, N. (2002). Accepted for publishing in *J. Mag. Mag. Mat.*
- [10] Movchan, V.I., Grudeva, N. A. (1983). *Russ. Metall.*, 1, p. 121.
- [11] Movchan, B.I. and Vladimirova, V.V. (1982). *Izv. Akad. Nauk SSSR, Met.* (in Russian), 4, p. 91.
- [12]. Kowalik, J.A. and Marder, A.R. In *Proc Phase Transformation'87*, Cambridge, July 1987. The Institute of Metals, 1988; ed. Lorimer, G.W., p. 482.
- [13] Okita, T., Tomita, T., Nakaoka, K. (1984). *Tetsu-to-nagane* (in Japanese), 70, 1984, p. 2120.
- [14] Kim, K., Beynon, J.H. and Sellars, C.M. (2001). *Scripta Mater.*, 44, p. 141.
- [15]. Mogutnov, B.M., Emeljanenko, L.P., Kononov, A.A., Rogov, A.I. and Shvartsman L.A. *Physical chemistry of electrical steel treatment processes* (in Russian). Moscow: Metallurgija, 1990.
- [16] Wagner, C. (1952). *J. Metals*, 4, p. 91.
- [17] Swisher, J.H. (1968). *Trans. Metall. Soc. AIME*, 242, p. 763.
- [18] Pyyry, J., Kettunen, P. (1973). *Scand J. Met.*, 2, p. 265.
- [19] Smith, R.P. (1962). *Trans. Metall. Soc. AIME*, 242, p. 105.
- [20] Marder, A.R., Perpetua, S.M., Kowalik, J.A. and Stephenson, E.T. (1985). *Metall. Trans. A*, 16A, p. 1160.
- [21] Block, W.F., Jayaraman, N. (1986). *Mat. Sci. Tech.*, 2, p. 23.
- [22] Kovač, F., Nižník, S. (1996). *Kovové Materiály* (in Slovakian), 34, p. 105.
- [23] Rollett, A.D., Storch, M.L., Hilinski, E.J. and Goodman, S.R. (2001). *Metall. Mat Trans A*, 32A, p. 2001.
- [24] Kestens, L., Jonas, J.J., van Houtte, P. and Aernoudt, E. (1996). *Metall. Mat Trans A*, 27A, p. 2347.
- [25] Kawamata, R., Kubota, T. and Yamada, K. (1997). *JMEPEG*, 6, p. 701.